Electronic supplementary information

Au-catalyzed Monodisperse Colloidal Cu nanorods with Widely Tunable Surface Plasmon Resonances

Ying Li,[a] Chengzhou Zhang,[a] Xin Wu,[a] Xinyu Wang,[a] Juan Xu,*[ab] and Caixia Kan*[ab]

a College of Physics, Nanjing University of Aeronautics and Astronautics, Nanjing 210016, P. R. China.

b Key Laboratory of Aerospace Information Materials and Physics (NUAA) MIIT, Nanjing 211106, China.

*Corresponding author E-mail: xujuan@nuaa.edu.cn, cxkan@nuaa.edu.cn.

Experimental section

1. Chemicals

$HAuCl_4 \cdot 3H_2O$ (99%), $NaBH_4$ (98%), trisodium citrate (99%), ascorbic acid (99%), $AgNO_3$ (99%), Poly(vinylpyrrolidone) (Mw = 1300 000) and 4-nitrophenol (4-NP, 98%) were purchased from Sigma-Aldrich. Hexadecylbenzyldimethylammonium chloride (HDBAC, 95%), hexadecylamine (HDA, 95%) were obtained from TCI. Copric chloride dihydrate ($CuCl_2 \cdot 2H_2O$, 98%), glucose (98%), cetyltrimethylammonium chloride (CTAC, 97%), cetyltrimethylammonium bromide (CTAB, 99%), hydrochloric acid (HCl, 36-38 wt% in water), sodium oleate (NaOL, >95%) were purchased from Aladdin Reagent. Deionized water with a resistivity of 18.2 M cm produced by a Direct-Q 5 ultraviolet water purification system was used in all experiments.

2. Preparation of Au decahedral nanoparticles

The Au decahedral nanoparticles were grown through seed-mediated growth in aqueous solutions with reference to the previous procedure. Briefly, a freshly prepared, ice-cold $NaBH_4$ solution (0.625 mL, 0.01M) was injected quickly into an aqueous solution that was pre-made by mixing together $HAuCl_4$ (0.25 mL, 0.01 M), trisodium citrate (0.5 mL, 0.1 M) and CTAC (10 mL, 0.05 M). The resultant solutions were kept in an isothermal oven at 90℃ for 1.5 h for the growth of Au seeds. The seed solution (3 mL) was injected into the growth solution that was made in advance by mixing together HDBAC (100 mL, 0.1 M), $HAuCl_4$ (1 mL, 0.05 M) and ascorbic acid (0.75 mL, 0.1 M), followed by intense stirring for 30 s. The reaction solution was left undisturbed overnight at room temperature.

3. Preparation of Cu NRs

A total of 42 mg of $CuCl_2 \cdot 2H_2O$, 50 mg of glucose, and 0.24 g HDA were dispersed in 20 mL deionized water in room temperature. The mixture was stirred for 12 h to form a sky-blue homogeneous emulsion. 3 mL of as-prepared Au decahedral nanoparticles were injected into the solution followed by intense stirring for 5 min. The mixture was kept at 110 ℃ for 3 h under gentle stirring, and the color of the solution changed gradually to reddish brown. The diameter and length of the Cu NRs could be adjusted through changing the size or volume of Au decahedral

nanoparticles with reaction.

4. Preparation of Au NRs.

The seed solution for Au NRs was prepared by adding an ice-cold $NaBH_4$ solution (0.01 M, 0.6 mL) into a mixed solution of $HAuCl_4$ (0.05 M, 0.05 mL) and cetyltrimethylammonium bromide (CTAB) solution (0.1 M, 9.95 mL) under vigorous stirring at room temperature (30℃) for 2 min. The seed solution was aged at room temperature for 2 h before use. To prepare the growth solution, 0.9 g of CTAB and 0.1234 g of NaOL were dissolved in 50 mL of deionized water at 65℃ and then stirred at 200 rpm at room temperature for 3h for complete dissolution. 0.48 mL of 20 mM $AgNO_3$ solution was added and kept the mixture left for 15 min. 0.25 mL of 0.1 M $HAuCl_4$ solution was added and kept the mixture stirring at 200 rpm for 90 min. Then, 0.16 mL of HCl (36-38 wt.% in water) was injected. After another 15 min of slow stirring (200 rpm), 80 μL of 0.1 M AA was added and the solution was vigorously stirred for 30 s. Finally, 80 μL of seed solution was injected into the growth solution. The resultant solution was shaken for 30 s and then left undisturbed at room temperature for 12 h.

5. Catalytic property measurement of nanocatalysts

The catalytic efficiencies of nanocatalysts were assessed using the model reduction reaction of 4-NP reduced by $NaBH_4$. Firstly, the reaction was performed in the dark at room temperature and was measured by in situ measurement of UV-visible absorption spectram. A desired amount of nanocatalysts was added to 2 mL 4-NP solution (0.1 mM), and the mixed solution was vigorously stirred for 2 min. Then, the absorption spectram were recorded at short intervals to monitor the process of the reaction in the spectral range of 250–500 nm after adding 1 mL freshly prepared $NaBH_4$ (0.1 M) solution. The catalytic reaction rates of the reduction process were decided through calculating the changes in absorbance at 400 nm as a function of time. To understand the SPR effect on the catalytic reaction, 980 nm laser was employed as the excitation source to illuminate the catalysts during the catalytic processes, in which the power intensity was adjusted to 8 mW/cm^2.

6. First-principles calculations

First-principles calculations were performed within the framework of density functional theory

(DFT) using the CASTEP module[1, 2]. Surface slab models were constructed, and 2.0 nm vacuum layers were introduced normal to the surface to eliminate spurious interactions arising from periodic boundary conditions. The electronic structure was described using a plane-wave basis set with a kinetic energy cutoff of 571.4 eV, in conjunction with ultrasoft pseudopotentials within the generalized gradient approximation (GGA)[3]. Structural optimizations were carried out using the Broyden-Fletcher-Goldfarb-Shanno (BFGS) algorithm [4] until convergence criteria of 1×10^{-6} eV per atom for total energy, 0.03 eV $Å^{-1}$ for atomic forces, 0.05 GPa for stress, and 0.001 Å for atomic displacements were satisfied. All calculations were performed in reciprocal space. The adsorption energy was calculated as follows: [5, 6]

$$E_{ads} = E_{total} - E_{slab} - E_{adsorbate}$$

where E_{total}, E_{slab}, and $E_{adsorbate}$ represent the total energy of the adsorbate-slab system, the energy of the clean slab, and the energy of the isolated adsorbate in vacuum, respectively.

7. FDTD simulations

FDTD simulations were performed using FDTD Solutions 8.7 (Lumerical Solutions). During the simulations, an electromagnetic pulse in the spectral range from 300 nm to 1400 nm was launched into a box containing a target nanostructure. A mesh size of 1 nm was employed in calculating the extinction spectra and charge distribution contours of the Cu NRs and Au NRs. The refractive index of the surrounding medium was set at 1.33, that of water. The dielectric function of Au was obtained by fitting the measured data of Johnson and Christy, and that of Ag was fitted from Palik's data. The sizes of the Au NBPs and Ag NPs were set according to the average waist widths and lengths measured from the TEM images. The diameter and length of the Cu NRs were set at 30 nm and 140 nm, respectively. The diameter and length of the Au NRs were set at 16 nm and 80 nm, respectively. Because we were interested in the variation behaviors of the longitudinal plasmon peak position, the excitation light direction was set to be perpendicular to the length axis, with the electric field aligned along the length axis.

8. Characterization

The extinction spectra were measured on a Shimadzu UV-3600 Plus ultraviolet/visible/near infrared spectrophotometer. TEM imaging was carried out on a FEI Tecnai 12 microscope operated at 120

kV. SEM imaging was performed on an FEI Quanta 400 FEG microscope operated at 10 kV. HRTEM imaging, HAADF-STEM characterization and elemental mapping were performed on a FEI Tecnai F20 microscope operated at 200 kV and equipped with an Oxford energy-dispersive X-ray analysis system. X-ray diffraction (XRD) was performed using a Panalytical Empytean diffractometer.

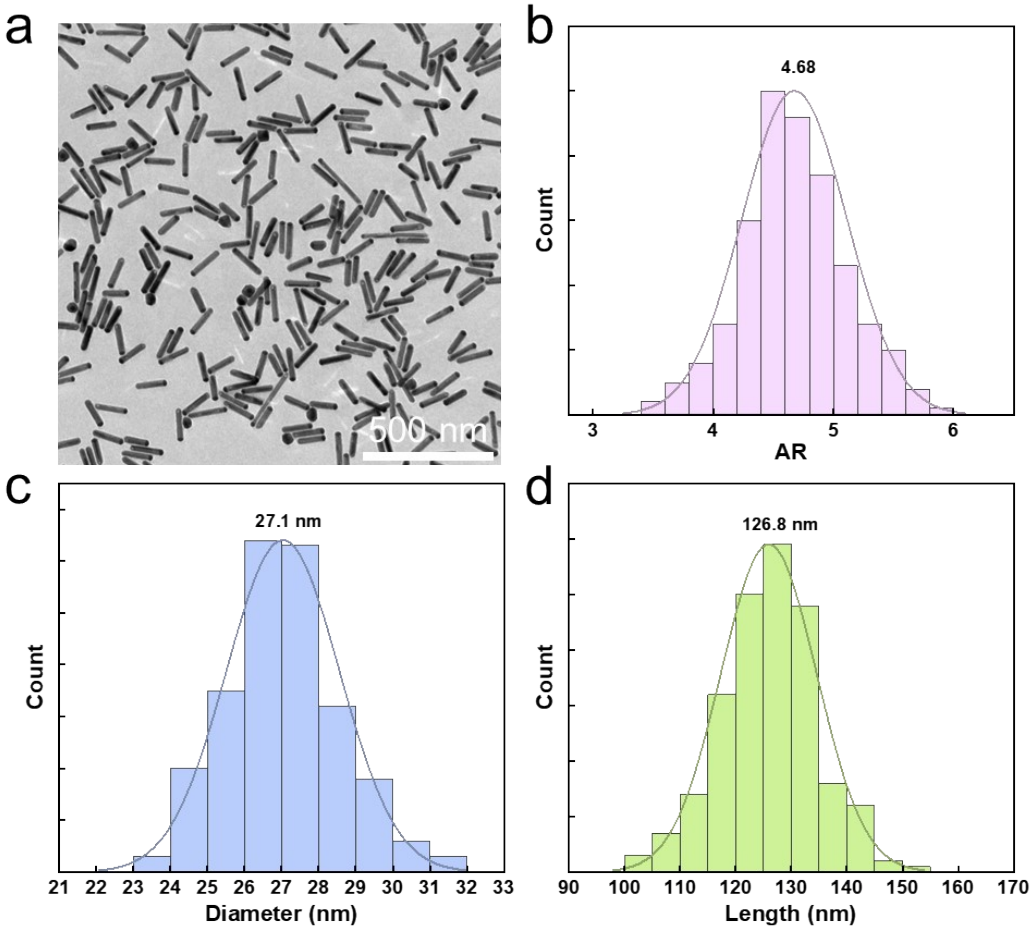

Fig. S1 (a) TEM image of Cu NRs. (b) AR distribution. (c) Diameter distribution. (d) Length distribution.

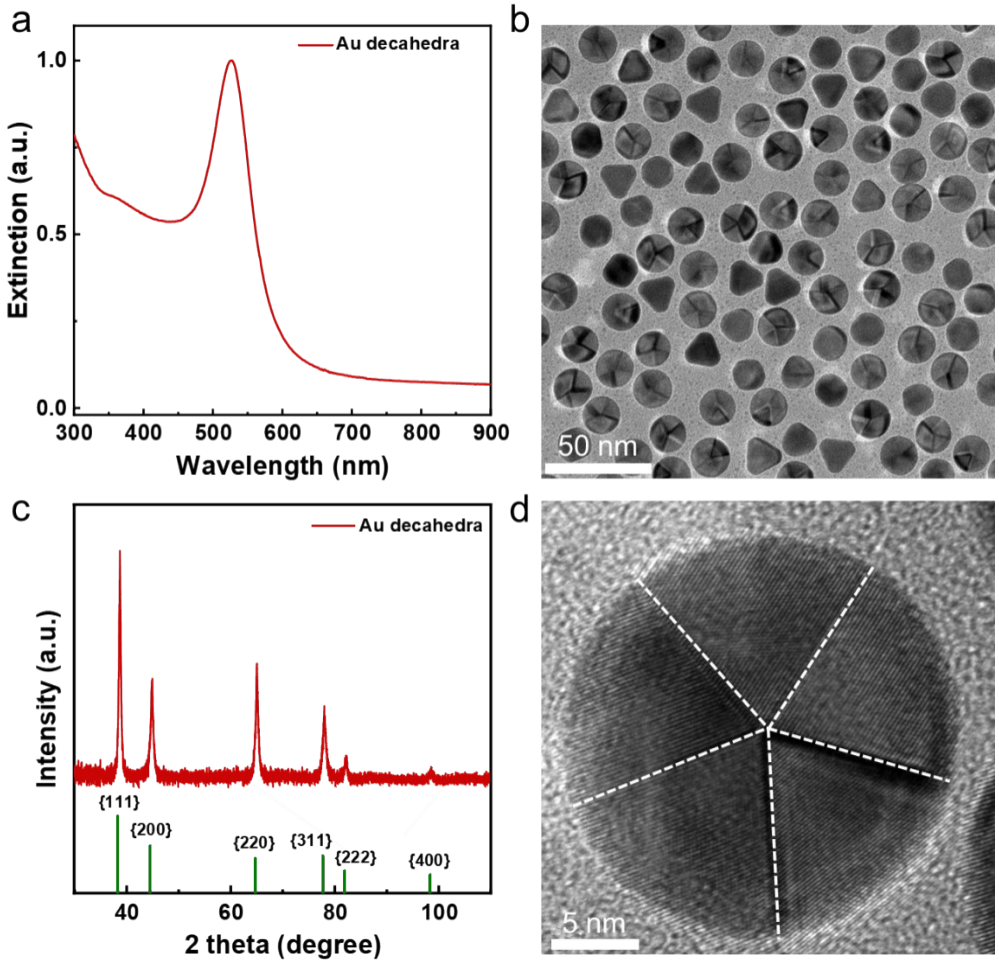

Fig. S2. Characteristic of Au decahedra. (a) Extinction spectrum and (b) TEM image of Au decahedra. (c) XRD patterns of Au decahedra. The vertical bars at the bottom represent the standard diffraction patterns of Au (JCPDS card no. 00-004-0784). (d) HRTEM image of a penta-twinned Au decahedron.

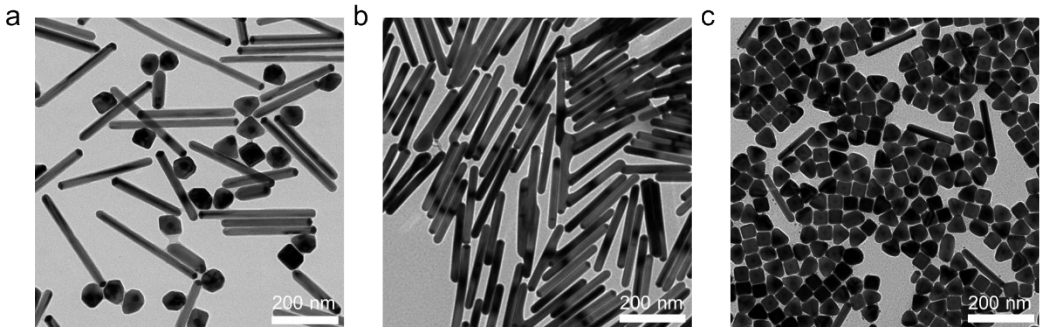

Fig. S3. TEM images of Cu NRs (a) before and (b) after purification. (c) TEM image of the impurity among purification process.

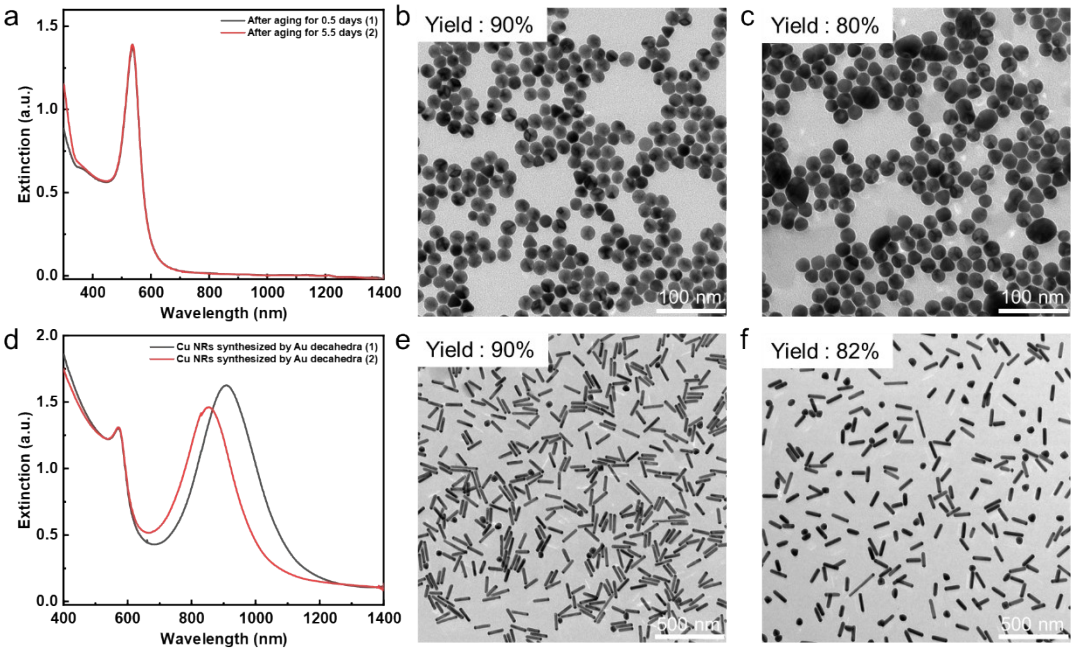

Fig. S4 (a) Extinction spectra of products obtained from growth solutions after aging for 12 h (1) and 5.5 days (2). (b-c) TEM images of products after aging for 12 h (b) and 5.6 days (c). (d) Extinction spectra of Cu NRs grown with Au decahedra with different aging times. (e-f) TEM images of Cu NRs synthesized by using Au decahedra aged for 12 h (e) and 5.5 days (f) as seeds.

Table S1. Synthetic parameters of Cu NRs.

Injection volume of Au seed solution (mL)	Injection volume of Au decahedra solution (mL)	Diameter of Cu NRs (nm)	Length of Cu NRs (nm)	Aspect ratio of Cu NRs
2 mL	40 mL	37 ± 4	150 ± 15	4.05 ± 0.6
4 mL	40 mL	29 ± 5	125 ± 16	4.13 ± 0.8
6 mL	45 mL	26 ± 4	111 ± 15	4.25 ± 0.6
6 mL	40 mL	26 ± 4	120 ± 20	4.59 ± 0.9
6 mL	35 mL	26 ± 4	126 ± 24	4.75 ± 1.2
6 mL	30 mL	26 ± 4	134 ± 20	4.95 ± 1.1
6 mL	25 mL	26 ± 4	139 ± 25	5.35 ± 1.2
6 mL	20 mL	26 ± 4	146 ± 30	5.71 ± 1.7
4 mL	30 mL	29 ± 5	169 ± 27	5.85 ± 2.1
4 mL	27 mL	29 ± 5	177 ± 25	5.96 ± 2.1
4 mL	24 mL	29 ± 5	189 ± 21	6.28 ± 1.5
10 mL	30 mL	17 ± 4	108 ± 28	6.45 ± 2.5
10 mL	25 mL	17 ± 4	114 ± 25	6.61 ± 2.6
10 mL	20 mL	17 ± 4	120 ± 31	6.85 ± 3.1
4 mL	20 mL	29 ± 5	211 ± 31	7.02 ± 2.9
4 mL	15 mL	29 ± 5	249 ± 30	8.32 ± 3.3

In this reaction, $NaBH_4$ was added in large excess, allowing its concentration to remain essentially constant throughout the reaction, such that the overall process could be treated as pseudo-first-order kinetics. The catalytic rate was determined by monitoring the time-dependent decrease in the characteristic absorption peak of 4-NP at approximately 400 nm. According to previous reports, 4-NP exhibits a strong absorption near 317 nm in neutral or mildly acidic aqueous solution. Addition of excess $NaBH_4$ induces deprotonation, causing a red shift to ~400 nm and a rapid color change from pale to deep yellow. Upon introducing the synthesized Cu NRs, the ~400 nm peak gradually decreased while a new peak at ~300 nm, corresponding to 4-AP, appeared and intensified, indicating efficient catalytic reduction of 4-NP to 4-AP.

In each reaction system, a good linear relationship was observed between the relative

absorbance $\ln(C_0/C_t)$ (where C_t is the concentration of 4-nitrophenol at time t) and the reaction time. Accordingly, the reaction rate constant (k) was obtained from the slope of the corresponding linear fit.

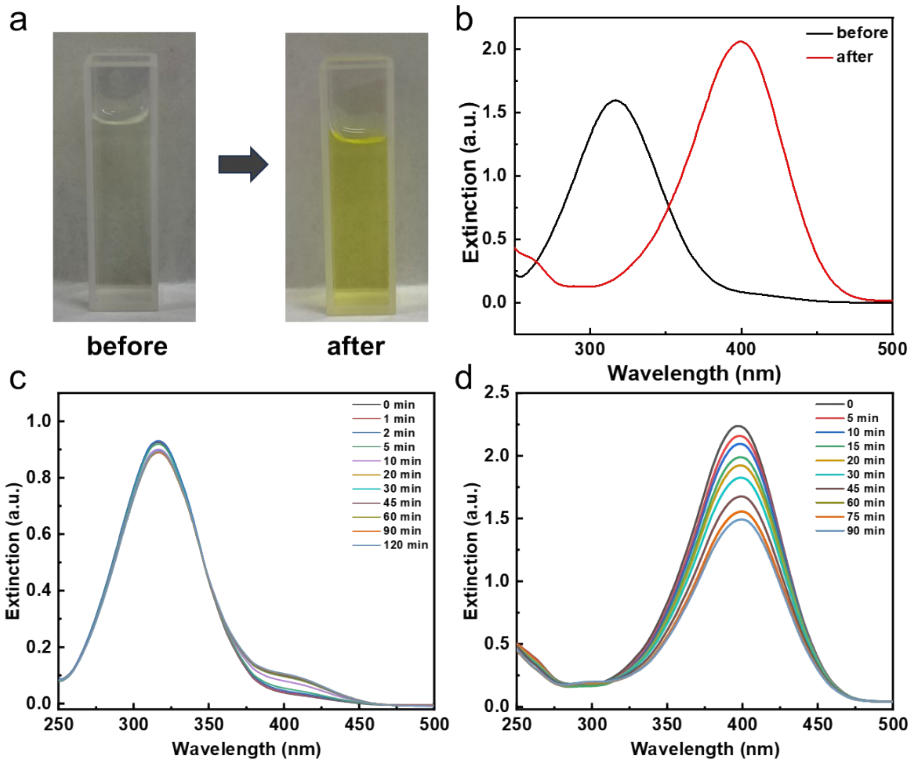

Fig. S5. (a) Color changes for 4-NP solution before and after the addition of $NaBH_4$. (b) Extinction spectra of 4-NP before and after the addition of $NaBH_4$. (c) Extinction spectra of 4-NP without $NaBH_4$ in the presence of Cu NRs. (d) Extinction spectra of 4-NP reduced by $NaBH_4$ without catalyst.

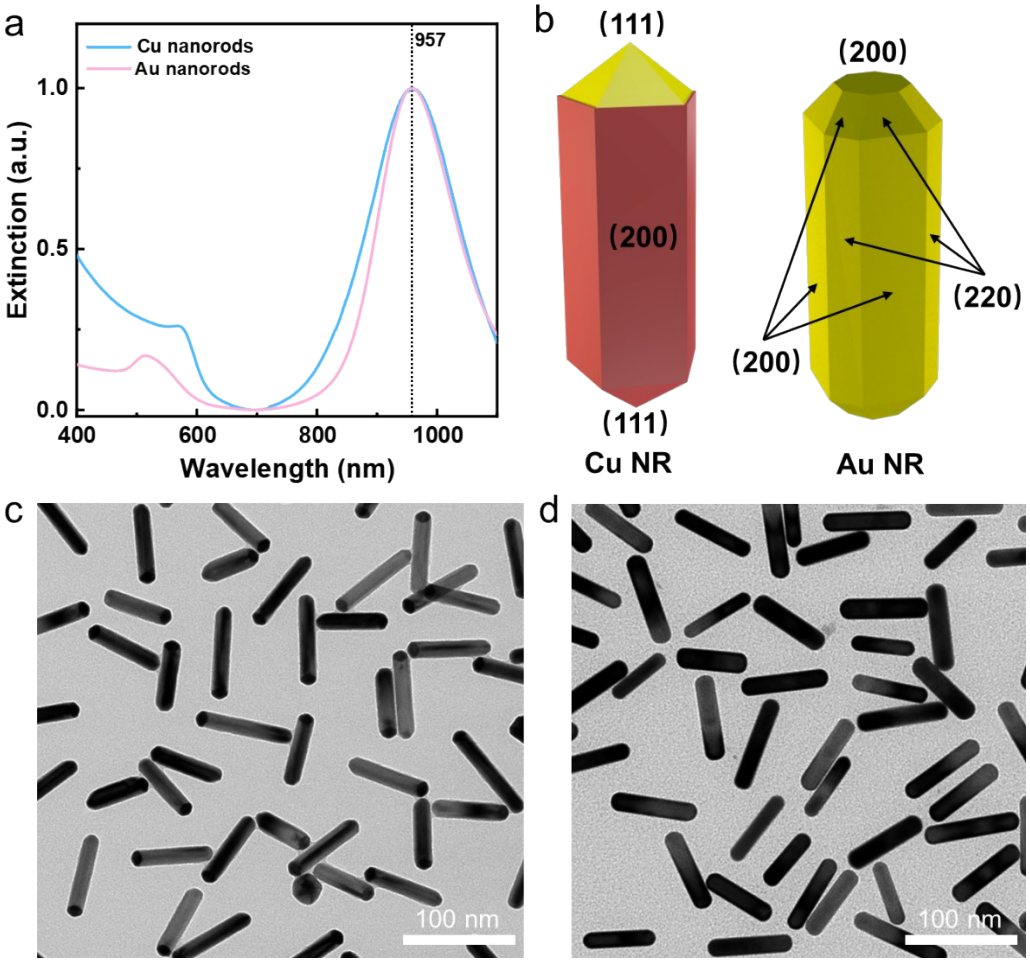

Fig. S6 (a) The extinction spectra of Cu NRs and Au NRs with SPR_L tunable at ~ 957 nm. (b) Schematic illustrations for facets of Cu NR and Au NR. (c) TEM image of Cu NRs. (d) TEM image of Au NRs.

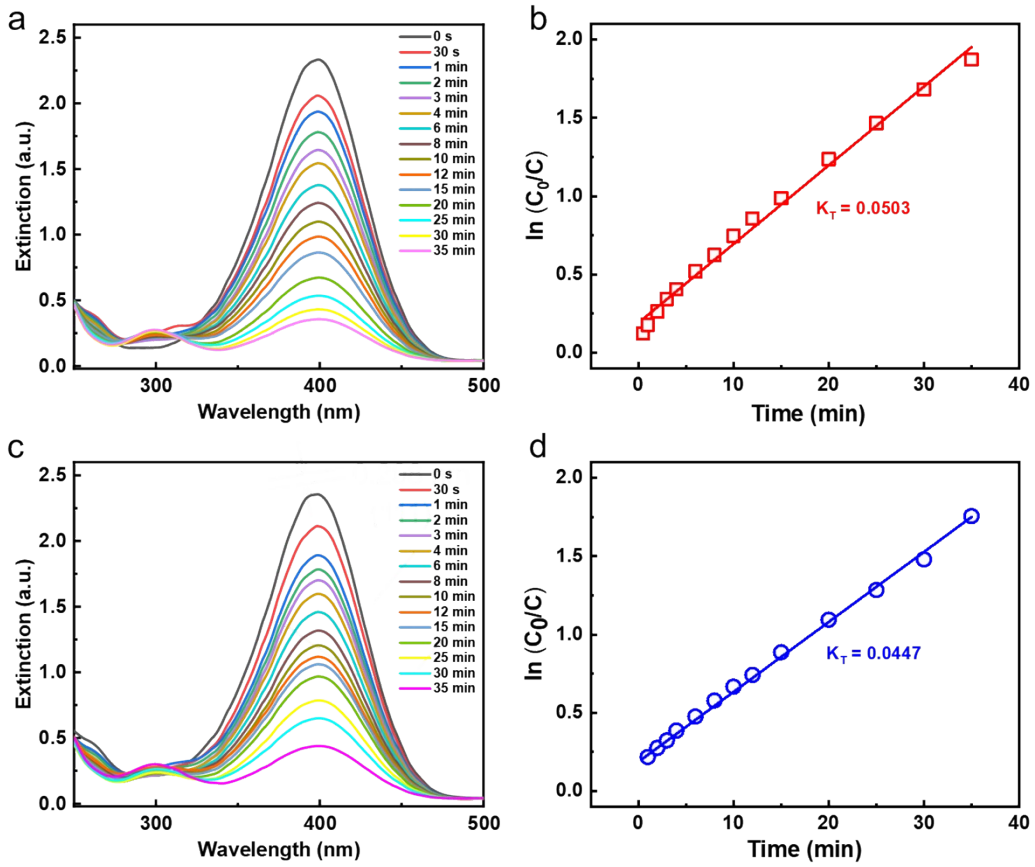

Fig. S7. Extinction spectra of 4-NP reduced by $NaBH_4$ in the presence of Cu NRs and Au NRs and $\ln(C_0/C_t)$ vs time plot for determination of rate constants of these NPs. All results were obtained in the dark under 300 K. (a, b) Cu NRs, (c, d) Au NRs.

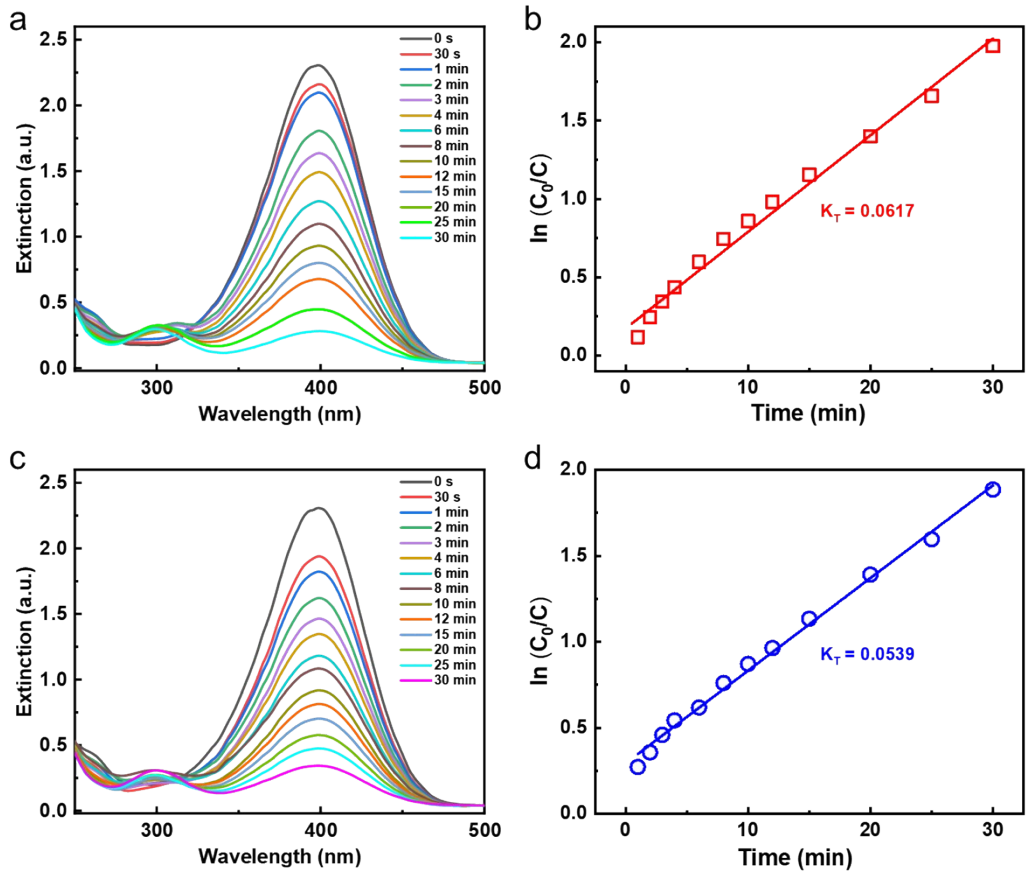

Fig. S8. Extinction spectra of 4-NP reduced by $NaBH_4$ in the presence of Cu NRs and Au NRs and $\ln(C_0/C_t)$ vs time plot for determination of rate constants of these NPs. All results were obtained under excitation at 980 nm. (a, b) Cu NRs, (c, d) Au NRs.

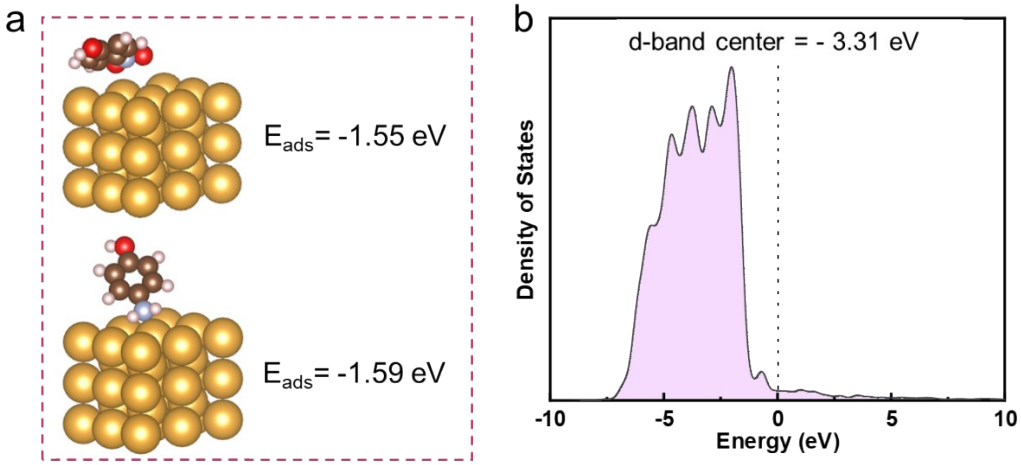

Fig. S9. (a) Front view of adsorption configurations and adsorption energies of 4-NP (top) and 4-AP (bottom) on Au (220). (b) Calculated DOS of Au (220).

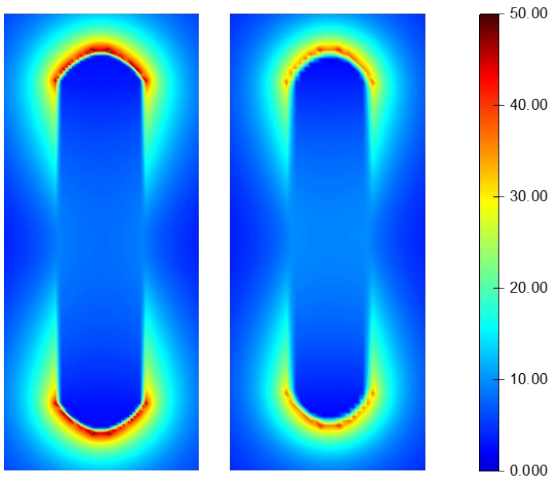

Fig. S10. Simulated electric field enhancement contours under the longitudinal excitation at 980 nm for the Cu NRs (left) and Au NRs (right).

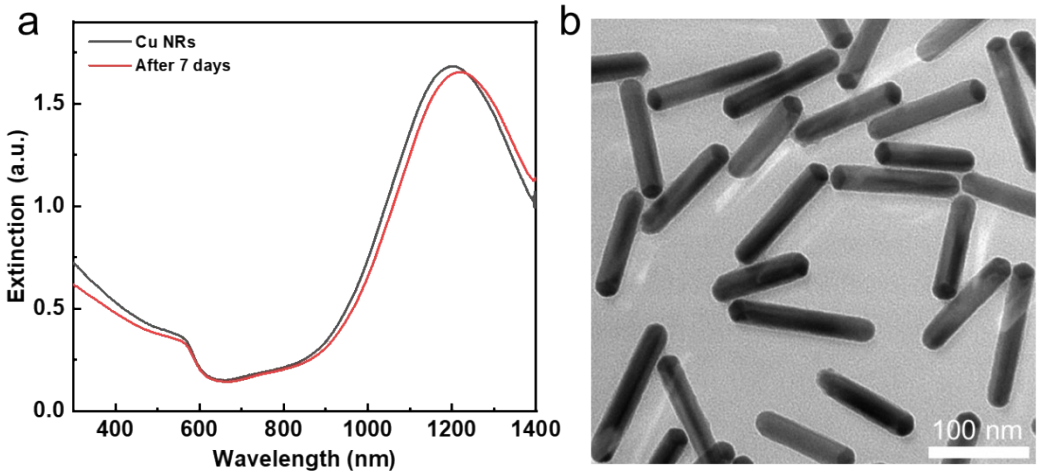

Fig. S11. Comparison of extinction spectra of Cu NRs before and after placing for7 days. (b) TEM image of Cu NRs after being placed for 7 days.

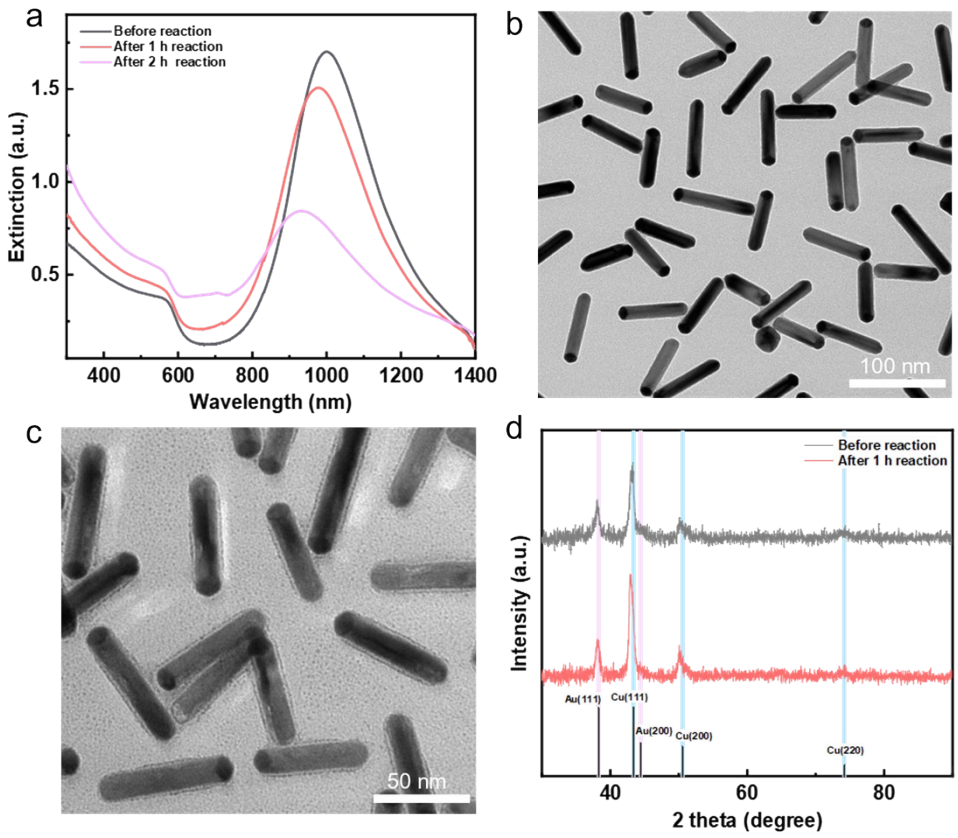

Fig. S12. (a) Extinction spectra of Cu NRs before and after the catalytic reaction. (b-c) TEM images for Cu NRs before (b) and after 1 h of (c) the catalytic reaction. (d) XRD patterns of Cu NRs before and after the catalytic reaction.

1. M. Segall, P. J. Lindan, M. a. Probert, C. J. Pickard, P. J. Hasnip, S. Clark and M. Payne, *Journal of physics: condensed matter*, 2002, **14**, 2717.
2. S. J. Clark, M. D. Segall, C. J. Pickard, P. J. Hasnip, M. I. Probert, K. Refson and M. C. Payne, *Zeitschrift für kristallographie-crystalline materials*, 2005, **220**, 567-570.
3. J. P. Perdew, K. Burke and M. Ernzerhof, *Physical review letters*, 1996, **77**, 3865.
4. B. G. Pfrommer, M. Côté, S. G. Louie and M. L. Cohen, *Journal of Computational Physics*, 1997, **131**, 233-240.
5. C. Freysoldt, B. Grabowski, T. Hickel, J. Neugebauer, G. Kresse, A. Janotti and C. G. Van de Walle, *Reviews of modern physics*, 2014, **86**, 253-305.
6. C. Zhang, X. Fu and H. Wang, *Materials Today Communications*, 2024, **40**, 109994.